The *gem*-dimethyl effect on reactivities in cyclizations through tetrahedral intermediates. Cyclization of methyl-substituted methyl amides of 5-(*p*-nitrophenyl)hydantoic acids

Asen H. Koedjikov,[a] Iva B. Blagoeva,[a] Ivan G. Pojarlieff*,[a] and Anthony J. Kirby[b]

[a] *Institute of Organic Chemistry, Bulgarian Academy of Sciences, ul. Acad. G. Bonchev block 9, Sofia 1113, Bulgaria*

[b] *University Chemical Laboratory, Lensfield Road, Cambridge, UK CB2 1EW*

The cyclization of the title hydantoinamides, UA, to 3-(4-nitrophenyl)hydantoins, Hyd, is general-base catalysed. Reversible hydrolysis of the product hydantoin from the 2,3-dimethylhydantoinamide, 2-UA, above pH = 7 is a complicating feature. The rate profiles for cyclization comprise one acid-catalysed, two neutral and two hydroxide-catalysed regions in the pH-region 0–10. Solvent kinetic isotope effects indicate rate-determining expulsion of the methylamino group in the acid-catalysed reaction. These also agree with general-base catalysis at low pH being concerted with nucleophillic attack of the ureido group. At high pH the tetrahedral intermediate is in equilibrium with the reactants and the rate is limited by proton transfers producing $T^{\pm}$. The accelerations upon methyl substitution vary strongly with the various processes observed and may be explained in terms of a general *gem*-dimethyl effect increasing along the reaction coordinate from reagent through cyclic tetrahedral intermediate to final ring product. As the effects for the breakdown of the intermediate are opposite in the forward and reverse directions, this changes the partitioning ratio and in turn could change the rate-determining step.

Models mimicking bioorganic reactions need to react rapidly to permit their study under the mild conditions of interest. The *gem*-dimethyl or Thorpe–Ingold effect, the favouring of cyclisation upon alkyl substitution in the chain,[1] is a useful tool for accelerating reactions between the functional groups because of the presumably small perturbation of their intrinsic reactivity, the acceleration being due to steric strain. For example the attack of ureido anion on negatively charged carboxylate has been studied as a model of biotin action.[2] With respect to such applications, the cyclization of ethyl hydantoates,[3] UE, turned out to be an unusual case. The rate of acid-catalysed cyclization increased by a factor of *ca.* 30 upon successive introduction of each methyl group in compounds (**1**–**3**)-UE; the base-catalysed cyclization of **3**-UE was, however, slower than that of **2**-UE and, further, the mechanisms of cyclization of the two compounds were different.

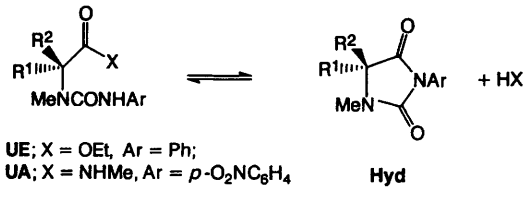

UE; X = OEt, Ar = Ph;
UA; X = NHMe, Ar = *p*-$O_2NC_6H_4$

Hyd

	R^1	R^2
1	H	H
2	Me	H
3	Me	Me

Evidently, for mechanisms established using sterically strained models to be relevant to their biological counterparts, their dependence on structure must be understood. One way to tackle this is to vary the functional groups in the open-chain compounds and observe the effect of alkyl substitution for a wider range of mechanisms.

We now report on the cyclization of the methylamides of 5-(*p*-nitrophenyl)hydantoic acids, compounds (**1**–**3**)-UA. Although altogether five reaction pathways could be detected in the pH-region studied, a 'normal' *gem*-dimethyl effect appeared to operate and no change of mechanism was observed. The difference in acceleration brought about by substitution for methyl in the various processes could be rationalised in terms of a general *gem*-dimethyl effect[4] increasing along the reaction coordinate. Opposite effects on the forward and the reverse breakdown of the tetrahedral intermediate can bring about a change of rate-determining step.

Experimental

Materials

Inorganic reagents and buffer components were of analytical grade and were used without further purification. Potassium hydroxide and buffer solutions were prepared with CO_2-free distilled water.

Heavy water was 99% D from Aldrich. Spectroscopic data for (**1**–**3**)-UA and (**1**–**3**)-Hyd are given in Tables 1–4.

2, *N*-Dimethyl-2-methylaminopropionamide

This was prepared from the respective methylamino ester[5] (0.5 g, 3.4 mmol) and methylamine (8.6 mmol as 40% water solution) by the procedure described for the *N*-methylamides of sarcosine[6] and of *N*-methylalanine.[7] After usual work-up 0.365 g (81%) of the amide was obtained as an amine-smelling oil (bp 95–100 °C at 20 mmHg). $\nu_{max}(CHCl_3)/cm^{-1}$ 3350 (NH), 1650, 1530 (amide); *m*/*z* 130 (M^+).

3, *N*-Dimethyl-5-(4-nitrophenyl)hydantoinamides

The title compounds were obtained by adding 2.9 mmol of *p*-nitrophenyl isocyanate dissolved in 10 cm^3 of dry benzene to a solution of 2.6 mmol of *N*-methylamide in 5 cm^3 of dry benzene with vigorous stirring and cooling with ice. A pale yellow solid precipitated immediately. Cooling was discontinued and the solution was stirred for a further 20 min. The solid was filtered off, washed with dry benzene and dried *in vacuo* over P_2O_5.

1-Methyl-3-(4-nitrophenyl)hydantoins

The title compounds were prepared by adding 4-nitrophenyl

Table 1 Data for *N*-Methyl-5-(4-nitrophenyl)-3-methylhydantoinamides[a]

Compound (Formula)	Yield (%)	Mp/°C	$m/z^+ + 1$	ν^{NHMe}/cm^{-1}	ν^{CO}_{urea}/cm^{-1}	ν^{CO}_{amide}/cm^{-1}	ν^{NH}_{amide}/cm^{-1}
1-UA $C_{11}H_{14}N_4O_4$	56	155–156	267	3275	1665	1650	1530
2-UA $C_{12}H_{16}N_4O_4$	80	75–77	281	3280	1660	1630	1530
3-UA $C_{13}H_{18}N_4O_4$	72	145–147	295	3360	1660	1650	1530

[a] IR spectra for samples in $CHCl_3$.

Table 2 ^1H NMR spectra of *N*-Methyl-5-(4-nitrophenyl)-3-methylhydantoinamides in $(CD_3)_2SO$, δ in ppm from Me_4Si splittings in Hz in parentheses

Compound	2-CH_3	*N*-CH_3 (amide)	*N*-CH_3 (urea)	2-H	2′-H	3′-H	N–H (amide)	N–H (urea)
1-UA		2.60d (4.5)	2.99s	3.93s	7.75d (9.3)	8.15d (9.3)	7.93q	9.10s
2-UA	1.27d (7.2)	2.59d (4.5)	2.89s	4.78q (7.2)	7.79d (9.2)	8.16d (9.2)	7.86q	9.07s
3-UA	1.335	2.52d (4.6)	2.98s		7.69d (9.3)	8.12d (9.3)	7.33q	9.00s

Table 3 Data for 1-methyl-3-(4-nitrophenyl)hydantoins[a]

Compound (Formula)	Yield (%)	MP/°C	$\nu^{C(2)O}/cm^{-1}$	$\nu^{C(2)O}/cm^{-1}$	Found (%) (Required) C	H	N
1-Hyd $C_{10}H_9N_4O_4$	75	164–165	1776	1724	50.90 (51.06)	4.08 (3.83)	17.82 (17.87)
2-Hyd $C_{11}H_{11}N_4O_4$	73	157–159	1777	1725	52.91 (53.01)	4.47 (4.42)	16.78 (16.86)
3-Hyd $C_{12}H_{13}N_4O_4$	68	174–175	1774	1723	54.67 (54.75)	4.99 (4.98)	15.93 (15.97)

[a] IR spectra for samples in $CHCl_3$.

Table 4 ^1H NMR spectra of 1-methyl-3-(4-nitrophenyl)hydantoins, in $(CD_3)_2SO$, δ in ppm from Me_4Si, splittings in Hz in parentheses

Compound	5-CH_3	1-CH_3	5-H	2′-H	3′-H
1-Hyd		3.12s	4.10s	7.75 (9.1)	8.32 (9.1)
2-Hyd	1.58d (6.9)	3.07s	4.10q (6.9)	7.77 (9.1)	8.33 (9.1)
3-Hyd	1.53s	3.00s		7.78 (9.1)	8.31 (9.1)

isocyanate (0.19 g, 1.2 mmol) to a solution of 1 mmol of the potassium salt of the respective methyl-substituted amino acid in 2.8 cm^3 of water. The mixture was stirred for 4 h at room temperature and left overnight. The *N*,*N*′-(4-nitrophenyl)urea formed was filtered off and the solution was acidified with an excess of conc. hydrochloric acid, refluxed for 3 h and left to crystallise. The hydantoins, (**1**–**3**)-Hyd were recrystallised from 2:1 ethanol–water. All three compounds gave satisfactory elemental analysis.

Kinetic measurements

Rate constants were determined at 25.0 ± 0.1 °C under pseudo-first-order conditions in the thermostatted cell compartment of a Unicam SP-800 or Carl Zeiss Jena UV–VIS spectrophotometer. The rate of cyclization of the ureido amides (**1**–**3**)-UA was followed by monitoring the decrease of absorbance at 330 nm. The reaction was initiated by injecting 20 μl of 0.01 mol dm^{-3} stock solution (DMSO) of the corresponding ureido amide to 2.80 cm^3 of preheated buffer solution. (Runs with **1**-UA were carried out in sealed ampoules.) Pseudo-first-order rate constants, k_{obs}, were obtained by non-linear-regression curve-fitting to the equation $A_t = A_0e^{-k_{obs}t} + A_\infty$ where A_t, A_0 and A are the absorbances at time, t, zero and infinity, respectively. The ionic strength was maintained constant (1.0 mol dm^{-3}) by potassium chloride. pH-values were measured directly after each kinetic run using a Radiometer pH M 84 Research pH-meter, with a GK 2401 C electrode standardized at pH 6.87, 4.01 and 9.18, respectively.

Experiments in D_2O solutions were run simultaneously with ones in H_2O of the same acid concentration in the multicell compartment of the spectrophotometer.

Equilibria between hydantoic acid and hydantoin in the case of **2**-UA were measured in several buffers starting from the hydantoin or from the potassium salt of the acid, which was obtained by hydrolysis at higher alkalinities from the hydantoin. In a solution of given pH, the same infinity readings at 330 nm were obtained at *ca.* ten half-lives.

Results

Machacek *et al.*[8] have shown that the base-catalysed ring closure of amides of hydantoic acids gives hydantoins but can sometimes be complicated by parallel hydrolysis of the amide group or by further hydrolysis of the product hydantoin.

The methyl amide of 5-(4-nitrophenyl)-2,2,3-trimethylhydantoic acid, **3**-UA, was converted quantitatively into the 3-(4-nitrophenyl)hydantoin **3**-Hyd over the whole pH range, studied by well-behaved pseudo-first-order kinetics and showed good isosbestic points when the complete spectra were recorded. The alternative possible reaction, attack of the amide group on the ureido function was excluded by the UV-spectra after ten half-lives. These were found to be identical with the 3-(4-nitrophenyl)hydantoin of the same concentration and not with

p-nitroaniline. With the dimethyl derivative **2**-UA the same was observed up to pH *ca.* 7. At higher pH the change of absorbance (at 330 nm) with time did not follow the pattern of single exponential decay and the infinity readings increased above those expected for the product hydantoin. Separate experiments showed that in this range the hydantoin, **2**-Hyd, hydrolyses reversibly to the hydantoic acid, **2**-A.

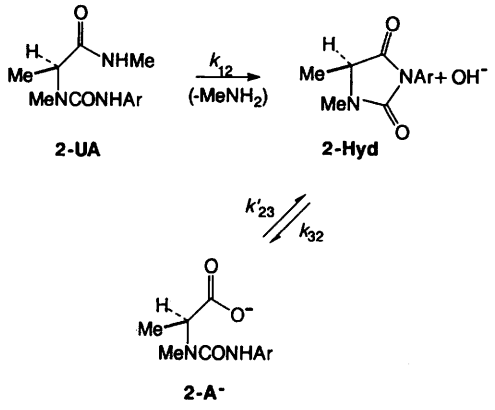

2-UA **2-Hyd**

2-A$^-$

The equilibrium constant, eqn. (1), was determined

$$K = \frac{k_{32}}{k_{23}} = \frac{[\text{Hyd}][\text{OH}^-]}{[\text{A}^-]} \qquad (1)$$

independently starting from the acid and from the hydantoin as 4.44×10^{-6} mol dm^{-3}. The rates of attainment of equilibrium in alkaline solution were similar to those for the cyclization of the amide but their ratio varied because the latter showed very strong buffer catalysis while the former did not. This complication of amide cyclization was accounted for by non-linear regression fitting the changes of absorbance with time to the integrated equation[9] for the above Scheme. Making use of the fact that the extinction coefficients of **2**-UA and **2**-A$^-$ were the same, this was used in the form of eqn. (2), where A is

$$A = A_{eq} + \frac{(\varepsilon_A C_0 + (a - c)\varepsilon_H C_0 - bq\varepsilon_A)e^{-at}}{b - a} + \frac{a(A_{eq} - \varepsilon_H C_0)e^{-bt}}{b - a} \qquad (2)$$

the absorbance, A_{eq} that at equilibrium; ε_A the extinction coefficient for **2**-UA and **2**-A$^-$, ε_H that for **2**-Hyd; and $q = (A_{eq} - \varepsilon_H C_0)/(\varepsilon_A - \varepsilon_H)$. The three fitted parameters, a, b and c are the observed first-order rates, k_{12}, $k_{23} + k_{32}$ and k_{32}, respectively.

A very good fit to the experimental data was obtained. In some of the experiments the observed A_{eq} was used; in the remaining ones, where the reaction was not followed to completion, the value calculated from the above equilibrium constant was used. The values for k_{12} appeared reliable (standard error not exceeding ± 1.5%). As expected, constant values for k_{32} were obtained [$(6 \pm 1.7) \times 10^{-5}$ s^{-1}] for 14 experiments in the most alkaline buffers starting from Tris 50% base.†

The rate of cyclization of **1**-UA was measured only in 1 M HCl because the reaction was too slow for a study of its rate profile to be practical.

The rate profiles for the cyclization of the hydantoic acid amides are shown in Fig. 1. These depict the rates measured in HCl solutions and also the rate coefficients, k_0 extrapolated to zero buffer concentration from the buffer experiments listed in Tables 6 and 7.‡ For the HCl solutions, activities instead of the usual convention of concentrations were used to bring these in line with the buffer data. An activity coefficient of 0.851 at I = 1 M KCl was used, determined from a linear dependence of pH against $-\log C_{H^+}$ for solutions of HCl with concentrations less than 0.3 M (slight curvature at higher HCl concentrations was attributed to the error arising from the glass electrode).

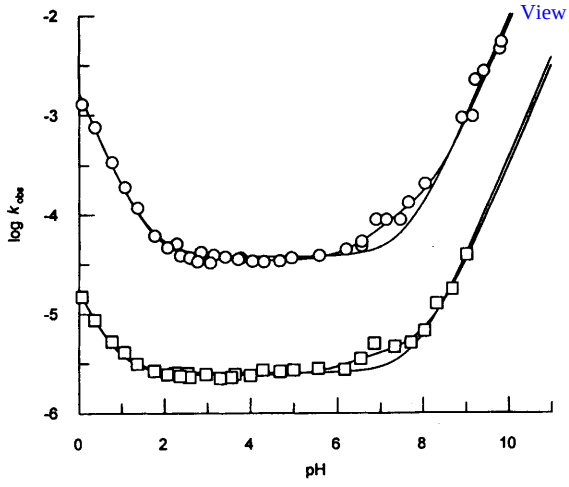

Fig. 1 Rate profiles for the cyclization of hydantoinamides **2**-UA (□) and **3**-UA (○); lines drawn (*a*) with eqn. (3) and parameters from Table 5 and (*b*) by means of a 'simple' equation with single neutral and base-catalysed reactions

When the data were fitted to a rate equation containing only terms 1, 0 and −1 order in H$^+$, a reproducible hump near pH 7 indicated a more complex course of the reaction (Fig. 1). The deviation is not large and to remove doubts that this is due to poor extrapolation because of the strong buffer catalysis in that region, rates were measured down to buffer dilutions compatible with the pseudo-first-order conditions.§ In order to test also whether this is not due to some unusual behaviour in phosphate buffers, data for **3**-UA in cacodylate and Tris buffers in the same pH region were collected and these confirmed the complication in the reaction profile. The rate data were fitted to eqn. (3).

$$\frac{V}{[\text{SH}]} = k_{obs} = k_H a_{H^+} + \frac{k_w + k^a_{OH} a_{OH^-} + k^b_{OH} k_d (a_{OH^-})^2}{1 + k_d a_{OH^-}} \qquad (3)$$

The second term of eqn. (3) can be obtained from eqn. (8) when k_2^H in the latter is neglected (justified under certain conditions—see the Discussion). The constants k_H were obtained separately from the data at lower pH and then fed into eqn. (3). The curves in Fig. 1 were calculated using the rate coefficients listed in Table 5.

The requirement for two different rate constants for OH$^-$-catalysis was supported by the different k_{OH} values obtained from curve-fitting to eqn. (4) (see below) of the rate data in buffers: those for **3**-UA were 465 and 704 in cacodylate and phosphate, respectively, and 76 in alkaline glycine buffer; for **2**-UA 33.6 and 2.55 in phosphate and Tris, respectively (all values in dm^3 mol^{-1} s^{-1}).

† One possible path of the reaction, in acid in particular, is hydrolysis of the amide function followed by rapid cyclization. One of the arguments against is the rate ratio **1** < **2** < **3** observed (Table 7), the opposite would be observed with hydrolysis of an open-chain amide.

‡ All observed pseudo-first-order rate constants are available from the British Library as deposited material, Supp. Publ. No 57167 (9 pp.).

§ In buffers with 10 or 90% base a higher limit to dilution had to be adopted (0.0064 M). The k_o-values for 10% carbonate and 90% phosphate showed strong positive deviations. As strict linearity was not observed in 90% phosphate and 10% carbonate buffers these values were discarded in constructing the rate profiles.

Table 5 Cyclization rates of methyl amides of 5-(4-nitrophenyl)hydantoic acids at 25.0 °C and I = 1 mol dm^{-3} (KCl)

Compound	$k_H/10^{-5}$ dm^3 mol^{-1} s^{-1}	$k_w/10^{-5}$ s^{-1}	k^b_{OH}/dm^3 mol^{-1} s^{-1}	k^a_{OH}/dm^3 mol^{-1} s^{-1}	$k_d/10^7$ dm^3 mol^{-1}
1-UA	0.0842 ± 0.0029				
2-UA	1.47 ± 0.18	0.241 ± 0.06	3.06 ± 0.23	171 ± 101	4.15 ± 2.76
3-UA	165 ± 20	3.45 ± 0.12	80.1 ± 5.0	1020 ± 411	0.976 ± 0.566

Table 6 Buffer catalysis of the cyclization of the methylamide of 2,3-dimethylhydantoic acid, **2**-UA, at 25.0 °C and ionic strength I = 1 mol dm^{-3} (KCl)

Buffer acid	% Base	Conc. range/mol dm^{-3}	No. of runs	$k_o/10^{-6}$ s^{-1}	$k^a_B/10^{-6}$ dm^3 mol^{-1} s^{-1} [a]
$H_3N^+CH_2CO_2H$	30	0.1–1	3	2.54	0.747 ± 0.094
	50	0.1–1	3	2.50	
	70	0.1–1	3	2.44	
	90	0.1–1	3	2.29	
HCO_2H	30	0.1–1	3	2.22	1.94 ± 0.24
	50	0.1–1	3	2.45	
	70	0.1–1	3	2.38	
CH_3CO_2H	30	0.1–1	3	2.69	5.89 ± 0.37
	50	0.01–1	4	2.61	
	70	0.01–1	4	2.69	
$H_2PO_4^-$	10	0.016–0.8	5	2.79	154[b] ± 15
	30	0.016–0.6	5	2.71	
	50	0.016–0.5	5	3.49	
	70	0.0032–0.4	8	4.97	
	90	0.0064–0.35	8	10.5[c]	
Tris	10	0.0064–0.008	2		2450[d] ± 450
	20	0.0032–0.008	3	5.07	
	30	0.0032–0.008	3	6.65	
	50	0.0032–0.008	3	12.5	
	70	0.0032–0.008	3	17.5	
	90	0.0064–0.008	2		
HCO_3^-	10	0.0064–0.8	7		79920[e] ± 8900
	20	0.0032–0.008	3	38.5	

[a] Obtained by means of eqn. (4) unless stated otherwise. [b] See the text, k_{OHB} = 811 ± 114 dm^6 mol^{-2} s^{-1}, from eqn. (4), k_{OH} = 33.6 ± 2.4 dm^3 mol^{-1} s^{-1}. [c] Calculated from data in the four most dilute buffers. [d] k_{OH} = 2.55 ± 0.34 dm^3 mol^{-1} s^{-1}. [e] From a linear regression ($k_{obs} - k^b_{OH}[OH^-]$) against [B].

Initially, the catalysis by the general acid or base was determined by fitting to eqn. (4), omitting either the k_H or the k_{OH} terms, or both where appropriate according to the observed rate profile.

$$k_{obs} = k_A[A] + k_B[B] + k_W + k_H a_{H^+} + k_{OH} a_{OH^-} \quad (4)$$

In some of the buffers, the pH varied considerably with total buffer concentration and plots of k_{obs} against total buffer concentration showed deviations from linearity. 'Buffer failure', *i.e.*, when the buffer ratio [A$^-$]/[AH] changes from that of added acid and salt because the amount of H$^+$ demanded by the ionization equilibria of the weak acid or base has to be provided by appreciable dissociation of the acid, was significant in the acid glycine buffers. With the latter the concentrations of the buffer components were corrected using an apparent pK for each buffer ratio: pK = −log([A$^-$]/[AH]) + pH where the ratio is that of the added acid and salt and the pH at [buffer] equal 1 M. In order to reduce the number of fitted parameters, k_W was fed in as a known constant (the value obtained from the rate profile) in cases where k_H or k_{OH} was also determined.

Only general-base catalysis (GBC) was found to be significant: observed values of k_A were generally small, less than 5% of k_B and in some cases negative (these negative values were also small and could arise from specific ion effects). Plots of k_{obs} *versus* [buffer] were generally linear; except at the highest buffer concentrations in phosphate (70 and 90% base) strong positive deviations were observed (see the Discussion).

In carbonate buffers, however, these plots were curved at low buffer concentrations and had the form expected from eqn. (5) which is obtained from Schemes 1 and 3 at high pH.¶

$$k_{obs} = \frac{k^b_{OH}k_{db}[OH^-]^2 + k^a_B k_{db}[OH^-][B] + k^b_B[B]^2}{k_{db}[OH^-] + [B]} \quad (5)$$

This together with the rate profile suggested that two GBC processes and a change of the rate-determining step are involved. The suggestion was supported by experiments with formate and acetate in Tris carrier buffers (10 and 30% base) where k_B constants for cyclization of **3**-UA 6–7 times larger were observed. The data on buffer catalysis are summarized in Tables 6 and 7.

The solvent kinetic isotope effects, k_H/k_D, for the ring closure of **3**-UA were measured for the k_H reaction in 0.95 M and 0.3 M HCl and DCl as 0.67 and 0.79, respectively, and for the k_w reaction in 0.002 M acids (I = 1 M, KCl) as 3.06.

Discussion

Mechanisms

Neutral and base-catalysed reactions. The neutral *p*-nitrophenylureido group is a weak nucleophile; the pK_a-value of *p*-nitrophenylurea itself[10] is 14, not greatly different from H_2O.

¶ Eqn. (5) is obtained similarly to eqn. (3) by including in eqn. (8) terms for the general base B and neglecting the terms not important at high pH.

Table 7 Buffer catalysis of the cyclization of the methyl amide of 2,2,3-trimethylhydantoic acid, **3**-UA, at 25.0 °C and ionic strength I = 1 mol dm^{-3} (KCl)

Buffer acid	% Base	Conc. range/mol dm^{-3}	No. of runs	$k_o/10^{-5}$ s^{-1}	$k_B/10^{-5}$ dm^3 mol^{-1} s^{-1} [a]
$H_3N^+CH_2CO_2H$	30	0.1–1	3	5.07	3.68[b] ± 0.26
	50	0.01–1	4	4.14	
	70	0.01–1	4	3.88	
	90	0.01–1	4	3.64	
HCO_2H	30	0.01–1	4	3.71	6.80[c] ± 0.64
	50	0.01–1	4	3.54	
	70	0.01–1	4	3.38	
CH_3CO_2H	30	0.01–1	4	3.34	12.4 ± 1.02
	50	0.01–1	4	3.39	
	70	0.01–1	4	3.64	
Me_2AsO_2H	70	0.0064–0.15	8	5.29	195[d] ± 5
	90	0.0064–0.0112	4	8.76	
$H_2PO_4^-$	10	0.016–0.8	5	3.84[e]	
	30	0.016–0.6	5	4.41[e]	
	50	0.016–0.5	5	4.47[e]	357[f] ± 27
	70	0.0032–0.4	8	8.83[e]	
	90	0.0064–0.35	7	12.9[g]	
Tris	10	0.0064–0.015	4	8.76[g]	
	20	0.0032–0.0256	4	13.0	2040[h] ± 49
	30	0.016–0.6	5	20.1	
H_3BO_3	40	0.016–0.1	3	95.3	1680[i] ± 180
HCO_3^-	10	0.0064–0.2	6	168[f]	
	20	0.0032–0.2	7	220[f]	161000[j] ± 12000
	30	0.0032–0.2	8	296[e]	
	50	0.0032–0.1	7	450[e]	
$H_3N^+CH_2CO_2^-$	20	0.0032–0.2	9	94.9[e]	50500[k,l] ± 1290
	50	0.0032–0.2	8	528[e]	

[a] Obtained by means of eqn. (4) unless stated otherwise. [b] k_H = (2.08 ± 0.29) × 10^{-3} dm^3 mol^{-1} s^{-1}. [c] k_H fed in as known. [d] k_{OH} = 465 ± 12 dm^3 mol^{-1} s^{-1}. [e] Determined from four points at lowest buffer concentrations. [f] See the text, k_{OHB} = 1330 ± 197 dm^6 mol^{-2} s^{-1}, from eqn. (4), k_{OH} = 704 ± 41 dm^3 mol^{-1} s^{-1}. [g] Determined from three points at lowest buffer concentrations. [g] k_{OH} = 169 ± 7 dm^3 mol^{-1} s^{-1}. [h] From k_{obs} corrected by means of eqn. (3). [i] Rate coefficient for observed buffer catalysis, in dm^3 mol^{-1} s^{-1}, at the buffer ratio shown. [j] Obtained as k_{bB} from eqn. (5), k_{OHB} = 43.4 ± 40.0, k_{db} = 2.71 ± 2.3. [k] Obtained as k_{bB} from eqn. (5), k_{OHB} = 30.5 ± 17.3, k_{db} = 2.57 ± 1.7. [l] From eqn. (4), k_{OH} = 76.0 ± 19 dm^3 mol^{-1} s^{-1}.

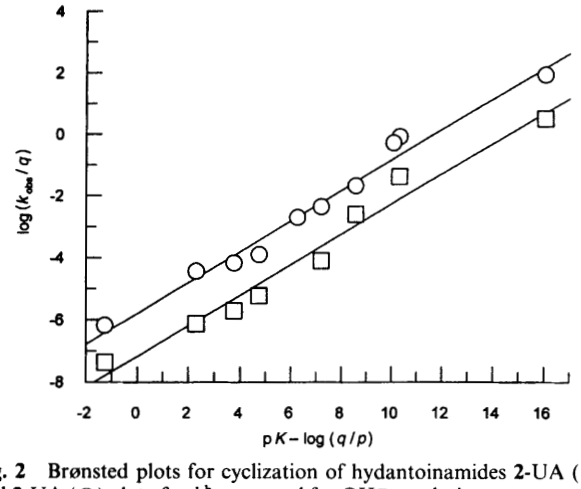

Fig. 2 Brønsted plots for cyclization of hydantoinamides **2**-UA (□) and **3**-UA (○); data for k_{OH}^b are used for OH^- catalysis

Current views on amide hydrolysis[11] and ester aminolysis[12] are thus relevant. Acylated amines as nucleophiles towards amides[13] or as leaving groups[14] upon aminolysis have also been studied.

pH–rate profiles of the type shown in Fig. 1 have been observed for acyl transfers through tetrahedral intermediates for ester aminolysis and other reactions.[15] The kinetics of such reactions have been analysed by Schmir.[15] Two neutral and two first-order regions in OH^- can be observed when the partitioning ratios of the intermediate for the neutral and base-catalysed reactions differ and the rate constants of the individual steps obey certain conditions. More recently DeTar[16] pointed out that Schmir's analysis does not apply when equilibrium is attained between the ionized forms of T. In the latter case the reactions go simply by the lowest energy path available to T^0 and T^-, respectively, which in turn corresponds to single 0th and 1st order in OH^- regions in the rate profile.[17]

As well as the rate profile, the mechanism must account also for the normal isotope effect of the water reaction in 0.002 M hydrochloric acid and for the buffer catalysis throughout the entire rate profile. All constants for GBC give reasonably good Brønsted plots which include the data for water and hydroxide anion, Fig. 2, the Brønsted β being *ca.* 0.50 for both compounds. A linear free-energy relationship encompassing the complete series is usually considered as evidence for a single mechanism,[18] the value of β indicating proton transfer concerted with heavy-atom reorganization. The complex pH–rate profile observed with the cyclization of ureido amides shows the dangers involved in such assumptions.

The interpretation of the kinetic results is simpler when one of the steps, formation or breakdown of the tetrahedral intermediate, is clearly rate determining. 4-Iminohydantoins are reported[19] to undergo hydrolysis below pH 7 to hydantoins, just as 2-thio-4-imino-3-phenyldihydrouracils give dihydrouracils in weakly acidic media but the amide of the thioureido acid

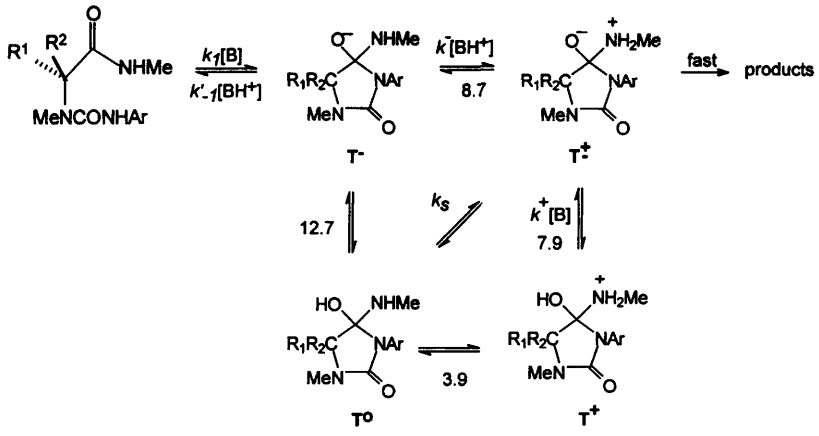

Scheme 1

in base.[20] With respect to the formation of the urea to carbon C–N bond and the rupture of the amide C–N bond this resembles the behaviour of alkyl acetates upon aminolysis by alkylamines: where C–OR bond cleavage is rate determining at low pH and formation of the C–N bond, actually related proton transfers, is rate determining at high pH.[12a]

Scheme 1 describes our preferred mechanism. The numbers given in Scheme 1 are the pK values estimated according to Fox and Jencks.‖[21] The recent procedure of Taylor[22] gave less consistent results. A pK value of 11.06 has been determined experimentally[23] for the related system (**4**).

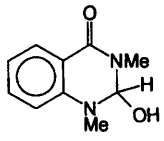

4

As already mentioned, the experimental data show GBC over the whole rate profile suggesting that both formation and breakdown of the tetrahedral intermediate, T, are GBC. When B = OH^-, the formation of T, will undoubtedly be a two-step reaction: fast deprotonation of the ureido group followed by attack of the anion, *i.e.*, specific base catalysis. When the base is water, deprotonation should still be faster than k_{obs} as estimated from the already mentioned pK of 14. This reaction is, however, more than 15 pK units uphill and we believe that for this reason for water catalysis k_1 favours the concerted path whereby deprotonation is coupled with N–C formation. Analogous to the reverse reaction is aminolysis of acetylimidazole (pK_{AH} of neutral imidazole = 14.2) by strong amines where expulsion of the leaving group is general-acid catalysed.[24] A concerted mechanism may explain the solvent kinetic isotope effect, SKIE, of 3.06 and is supported by the fact that the first four points of the Brønsted plots (water and the weak bases: glycine, formate and acetate) give straight lines with slopes 0.35 for **2**-UA and 0.38 for **3**-UA (Fig. 2).

A SKIE of 3.05 is calculated for the k_W reaction using the procedures outlined by the Schowens.[25,26] The fractionation factors of the transition state were determined using $\beta = 0.38$, and assuming a fractionation factor of 0.4 for the proton in flight (following Brown[11b]).

The numbers in Scheme 2 show the fractionation factors different from unity. At high pH where breakdown of T is presumed rate-determining, GBC can likely be attributed to production of the unstable $T^{\pm}$.[12a] Scheme 1 can be conveniently recast as Scheme 3.

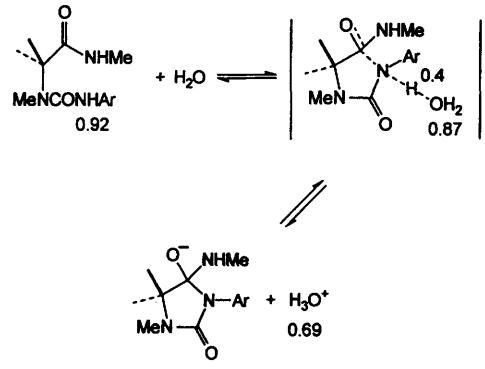

Scheme 2

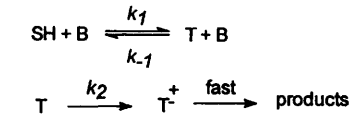

$[T] = [T^+] + [T^0] + [T^-]$;

Scheme 3

The steady state solution gives eqn. (6).

$$\frac{V}{[SH]} = k_{obs} = \frac{\sum_i k_1^i [B_i] \sum_i k_2^i}{\sum_i (k_{-1}^i [B_i] + k_2^i)} \qquad (6)$$

The definitions of the constants in Scheme 3 are mechanistically compatible with those of Scheme 1 providing there is a rapid equilibrium between the three forms of T. The k_1 processes produce T^-. The latter, with a pK of 12.7, will be protonated by water to T^0 with a rate close to the diffusion limit. While the k_1 constants of Scheme 3 are the same as those of Scheme 1, the k_{-1} constants are different: at pH-values where T^0 is prevalent they include the deprotonation equilibrium constant times the rate constant of the reverse breakdown of T^- of Scheme 1.

$$k_{-1}^i = k'_{-1} \frac{K_{T^0}}{K_{BH^+}}$$

The routes of conversion of T into $T^{\pm}$ include acid catalysis *via* T^+, a water-mediated switch from T^0, and base catalysis *via* T^- [eqn. (7)].

‖ The σ_I-values of Hansch, Leo and Taft (*Chem. Rev.*, 1991, **91**, 165) were used. The procedure is outlined in the deposited material.

$$k_2[T] = k^+[T^+][B] + k_s[T^0] + k^-[T^-][BH^+]$$

$$k_2 = \frac{k^+[H^+][B]}{[H^+] + K_{T+}} + k_s\frac{K_{T+}K_w/K_{T0}}{([H^+] + K_{T+})([OH^-] + K_w/K_{T^0})} + \frac{k^-[OH^-][BH^+]}{[OH^-] + K_w/K_{T^0}} \quad (7)$$

In the pH region 6–10 where k_2 becomes rate determining eqn. (7) can be simplified because the presence of T^+ and T^- is negligible. When the bases are only water and OH^- this gives eqn. (7a).

$$k_2 = \frac{k_H^+[H^+]}{K_{T+}} + \frac{k_w^+K_w}{K_{T+}} + k_s + k_w^+K_{T0} + \frac{k_{OH}^-K_{T0}[OH^-]}{K_w} \quad (7a)$$

The steady-state solution of Scheme 3 can then be presented as eqn. (8) where the pH-independent terms have been grouped

$$k_{obs} = \frac{(k_1^w + k_1^{OH}[OH^-])(k_2^w + k_2^{OH}[OH^-] + k_2^H[H_3O^+])}{k_{-1}^w + k_{-1}^{OH}[OH^-] + k_2^w + k_2^{OH}[OH^-] + k_2^H[H_3O^+]} \quad (8)$$

and denoted by superscript *w*, *etc.* Omission of the k_2^H terms** (v.i.) transforms eqn. (8) into the empirical eqn. (3), where $k_d = (k_{-1}^{OH} + k_2^{OH})/(k_{-1}^W + k_2^W)$, *etc.*

The pH-independent rate at low pH, k_W, is then equal to k_1^w to agree with evidence of rate-determining formation of T. Water and proton catalysis ensure the rapid conversion of T^0 to the unstable $T^\pm$. k_2^W is mainly k_s, the water-mediated proton switch from T^0 to $T^\pm$. This is estimated to be 10^2–10^3 s^{-1} since the reverse k_{-s} has been shown[11a] to be 10^6–10^7 s^{-1} and the equilibrium constant between T^0 and $T^\pm$ is seen on Scheme 1 to be about 10^{-4}, $k_s = k_{-s}K_s$. With a pK_{T^+} of 3.9 the term for proton catalysis becomes constant at pH values below that p*K*. This is actually the rate of deprotonation of T^+, an OH acid of p*K* 7.9, by water ($k^+[B]$), *ca.* 10^2 s^{-1} (using 10^{10} dm^3 mol^{-1} s^{-1} for the diffusion-controlled reaction).[27] The contribution being proportional to $[T^+]$ becomes negligible above pH 6 according to these estimates.

The rate coefficient for OH^--catalysis in the lower pH region is k_1^{OH}, the attack of ureido anion (experimentally k_{OH}^a). The condition for this is that upon increasing $[OH^-]$ only in the first term of the numerator does k^w become smaller than $k^{OH}[OH^-]$; in the denominator k_{-1}^w must be $< k_2^W(+k_2^H[H^+])$ for formation to be rate-determining at low pH. In contrast for breakdown of T to be rate-determining under basic conditions k_{-1}^{OH} must be greater than k_2^{OH} which means that the rate at the plateau at higher pH, k_{OH}^a/k_d, will be equal to $K_Tk_2^W$. K_T is the equilibrium constant as defined in Scheme 3. Similarly, the second OH^--reaction, k_{OH}^b, will have a rate constant equal to $K_Tk_2^{OH}$. The rate constant for OH^--catalysed breakdown, k_2^{OH},†† involves only proton transfers and is estimated to be 10^6 dm^3 mol^{-1} s^{-1} which, combined with k_{OH}^b, gives K_T *ca.* 8×10^{-5} for **3**-UA and 3×10^{-6} for **2**-UA. These values for K_T give a k_2^W of about 100 s^{-1} from the observed rates at the plateau at higher pH. A comparison with the above estimate of k_2^W as k_s shows good agreement.

To summarize, the pH–rate profile is interpreted in terms of the change in the rate-determining step taking place when the conversions of T^0 catalysed by OH^-, $(k_{-1}^{OH} + k_2^{OH})[OH^-]$, become faster than those catalysed by water, $k_{-1}^w + k_2^W$. This in turn is due to k_{-1}^{OH} being $> k_2^{OH}$, while $k_{-1}^w < k_2^W$. The changes in slope from 0 to 1 both at low and at high pH are caused by the simultaneous catalysis by water and OH^- of formation and breakdown of the tetrahedral intermediate, respectively.

The steady-state equation when general catalysis is included becomes more complex and only the observed behaviour will be discussed. As judged from the pH–rate profile the change from rate-determining formation to rate-determining breakdown of the intermediate takes place at about pH 7–8 with proton transfers leading to $T^\pm$ becoming rate determining above this value. According to the p*K* estimates T^0 is the predominant form between pH 5–10, and is about 10^4 times more prevalent than $T^\pm$ at equilibrium. The conversion of T^0 into $T^\pm$ can occur through T^+ or T^-. According to the p*K*-values of the various forms of T given in Scheme 1 the dividing line is somewhere p*K* = 7–8. For bases with p*K* above 7–8, the route through T^- is preferred because of the smaller difference between the respective p*K* values. This is the reaction attributed to GBC by Tris, carbonate and alkaline glycine buffers. With a pK_{T^-NH} of 8.9 and pK_{T^0} of 12.7 equilibrium with these bases will not be attained with respect to the first step and the rate will be limited by deprotonation of T^0. The observed Brønsted plots in this region are compatible with β changing from 1 to zero (OH^--catalysis).

The experiments with formate and acetate in carrier Tris buffers, 10 and 30% base are not readily interpreted as they pertain to a transitional part of the rate profile. The rate constants k_{buf} appear to be pH-independent, averaging 5.23×10^{-4} and 1.03×10^{-3} dm^3 mol^{-1} s^{-1} for formate and acetate, respectively. However, the observation that the catalysis in Tris carrier buffers is different from that in the buffers themselves strongly supports the interpretation of a change in the rate-determining step.

Catalysis by cacodylate and phosphate takes place in the transition zone. In most cases the observed buffer catalysis k_{buf} depends only on [B]. However, eqn. (6) predicts cross-terms (k_1k_2) that may be significant under certain conditions. With phosphate buffers a third-order process proportional to [B] and [OH] becomes important. Plots of k_{buf} against base fraction are concave upwards. This is probably related to the fact that $k_1^{OH}[OH^-]$ is still significant. The rate constants for phosphate catalysis in Tables 6 and 7 were obtained by adding a k_B and a k_{OHB} term to eqn. (3) and using the parameters from the pH–rate profile to account for effect of a_{OH^-}.

Plots of k_{obs} *vs.* [buffer] in carbonate are curved and suggest two parallel processes: one linear and one going to saturation. Such a course of the reaction is possible according to eqn. (5), which is obtained similarly to eqn. (8) from eqn. (6) taking into account only the terms important at high pH. However, reliable constants for the saturation process could not be obtained and are not discussed further.

Returning to the Brønsted plots on Fig. 2, slopes *ca.* 0.5, we consider their linearity to be fortuitous. The appearance of the plots is enhanced by the disposition of the points for water and OH^- catalysis. According to the mechanism suggested the points from water to acetate form part of a line, as already mentioned, of slope 0.4 characteristic of a concerted GBC formation of T^-; the data from Tris to OH^- are compatible with a slope changing from 1 to 0 expected for simple proton transfers, while the points for cacodylate and phosphate are intermediate.

Acid catalysed reactions. As mentioned already, the acid-base properties of the *p*-nitrophenyl-ureido group are similar to those of water and thus a mechanism similar to the acid-catalysed hydrolysis of amides becomes likely. Recent extensive studies by Brown[11] have confirmed that formation of the tetrahedral intermediate is rate determining. The preferred mechanism from solvent kinetic isotope effects (close to 1,

** T^- formed in the first process will protonate both on O and on N to a similar extent by all neutral acids of p*K* smaller than 8.7 under diffusion control thus giving products directly through $T^\pm$. H_3O^+, however, will produce mainly T^0 because of electrostatic acceleration. The exact route for the second step is not important under conditions of rate-determining k_1.

†† k_2^{OH} is $k_{OH}^-(K_T^0/K_W)$ where k_{OH}^- is the reaction of water with T^-.

calculated to be 1.1 by means of fractionation factors[22,23]) and potential energy diagrams is attack of water on the protonated amide aided by transfer of a proton to a second molecule of water.

The cyclization of **3**-UA in 0.95 M LCl showed a SKIE, k_H/k_D = 0.79 (0.67) which is a substantially lower value than 1.1, calculated in our case also for the similar attack of the ureido group on the protonated amide, aided by transfer of proton to a water molecule using the assumptions of Brown and co-workers. The above-mentioned results for the hydrolysis of 1-imino-2-thio-3-phenyldihydrouracil showed that at acidities above 0.01 M H^+ thioureido amide is produced as well as thiodihydrouracil, the fraction of the former increasing with acidity. Thus there is no indication for a preferred rate-determining step from the data obtained so far. A SKIE of 0.78, the same as observed experimentally, is calculated within the Brown's framework (0.3 for the reaction coordinate, $\varphi^* = 0.5$ for the proton in flight) for rate-determining breakdown of T^+ aided by a molecule of water as depicted in transition state **5**.

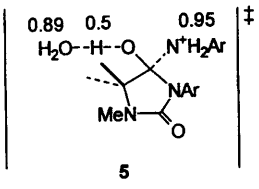

5

The *gem*-dimethyl effect on reactivity and mechanisms in cyclizations *via* tetrahedral intermediates

The accelerations of ring closure observed upon introduction of the third, geminal, methyl group vary between 112, 15 and 26 for k_H, k_W and k^b_{OH}, respectively (Table 5). Acid catalysis with **3**-UA appears at a_{H^+} *ca.* ten times lower than with **2**-UA (Fig. 1) reflecting the difference in these ratios; the *gem*-dimethyl effect improves the nucleophilicity of the *p*-nitrophenylureido group much more in the acid-catalysed than in the water reaction.

We have suggested previously[4] that it is useful to consider the *gem*-dimethyl effect as comprising two components: a general one measured by the effect of substituents on the equilibrium open chain ⇌ ring, and specific effects of some substituents due to interactions pertaining only to the transition state. The latter become apparent as deviations from linear free-energy relationships (rate against equilibrium constants). Although not easy to visualize, the *gem*-dimethyl effect results from release of strain upon cyclization roughly because bond eclipsing and bond angle changes in the ring allow more freedom to the substituents.[1] In ring closure of carboxylic acid derivatives through tetrahedral intermediates, the strain causing the general *gem*-dimethyl effect is gradually released along the various states because the intermediate with a tetrahedral carbon atom is expected to be more flexible than the final ring product with a trigonal carbon atom. Fig. 3 illustrates this trend; 2 is a more heavily substituted member of the series than 1.

According to Fig. 3 the largest effect is between reactants and products and will decrease as the state becomes closer to the reactants. Our mechanistic assignments fit the predictions of the diagram well. For acid catalysis SKIE data favour rate-determining k_2. The observed ratio of 112 then corresponds to the effect between the reactant R and the transition state $‡_{(2)}$. The water reaction shows a much smaller effect, a ratio of 15, expected between states R and $‡_{(1)}$ with rate-determining k_1. An intermediate ratio of 27 obtains for the constant k^b_{OH} assigned as $K_T k_2^{OH}$. This is again consistent because K_T is the equilibrium between R and T, while k_2^{OH} involves only proton transfers which should not be affected by the *gem*-dimethyl effect.‡‡

‡‡ The fourth constants k^a_{OH} were determined with a too great an uncertainty in order to discuss their ratio.

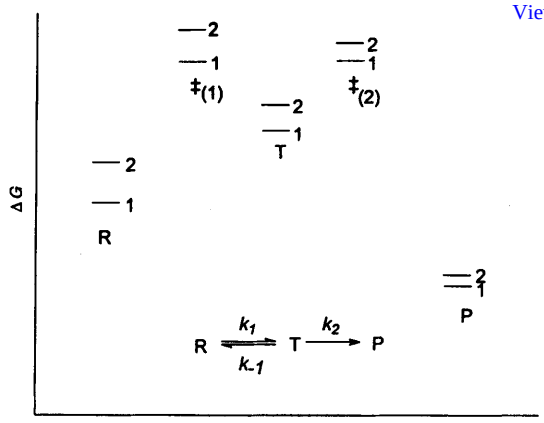

Fig. 3 Diagram of the free-energy changes expected from the *gem*-dimethyl effect for ring closure through a cyclic tetrahedral intermediate: 2 is a more heavily substituted member of the series than 1

The trends illustrated in Fig. 3 indicate an important possibility for a mechanism change with substitution from rate-determining breakdown to rate-determining formation of the tetrahedral intermediate. For Fig. 3, $k_{obs} = k_1k_2/(k_{-1} + k_{-2})$ and when k_{-1} is large and k_2 small the latter determines the rate, while in the opposite case k_1 is rate determining. In intermolecular reactions of open-chain compounds steric effects are generally believed to affect k_{-1} and k_2 similarly. In a reaction series in which the *gem*-dimethyl effect is operative the situation is completely different: the barrier for k_{-1}, from T to $‡_{(1)}$, increases with substitution, while that for k_2, from T to $‡_{(2)}$, decreases: the *gem*-dimethyl effect favours cyclization and hinders ring opening (k_{-1}). Thus if the reaction series sets out with rate-determining k_2, substitution can change that to rate-limiting k_1 provided k_2 becomes larger than k_{-1}. As far as rate-determining steps are concerned this is the change suggested[3] in the base-catalysed cyclization of ureido esters discussed in the introduction.

Earlier work[28] has shown considerable changes in the partitioning ratio for the dianion of the tetrahedral intermediate in the alkaline hydrolysis of 1,6-disubstituted dihydrouracils which could be attributed to an inverse *gem*-dimethyl effect. This is a ring-opening reaction and the general *gem*-dimethyl effect should decrease the partitioning ratio as was observed. In the most heavily substituted cases; the shape of the rate-profiles became different because a change in the rate-determining step was no longer observed.

For a change in mechanism to occur as a result of the general *gem*-dimethyl effect two conditions are apparently necessary: (*a*) upon cyclization increased substitution can shift the mechanism from rate-limiting breakdown to formation of the tetrahedral intermediate but not the reverse and (*b*) k_{-1} and k_2 should not be very different because the effects are probably not very large.

The hydantoinamides of this study, **2**-UA and **3**-UA, with respect to the neutral and basic reactions apparently do not fulfil the second condition because the two rate profiles are rather similar. However, the experimentally determined constant k_d [eqn. (3), Table 5], is smaller with **3**-UA than with **2**-UA in agreement with the above mechanistic assignments. When as assumed $k^w_{-1} < k^W_2$ and $k^{OH}_{-1} > k^{OH}_2$ then $k_d = k^{OH}_{-1}/k^w_2$. The latter inverse partitioning ratio should decrease with the general *gem*-dimethyl effect according to Fig. 3.

Acknowledgements

We thank the National Foundation for Scientific Research of Bulgaria for funding this research and the Bulgarian Academy of Sciences and The Royal Society for travel funds.

References

1 C. K. Ingold, *J. Chem. Soc.*, 1921, **119**, 305; C. K. Ingold, S. Sako and J. F. Thorpe, *J. Chem. Soc.*, 1922, 1117; N. L. Allinger and V. Zalkow, *J. Org. Chem.*, 1960, **25**, 701; I. B. Blagoeva, B. J. Kurtev and I. G. Pojarlieff, *J. Chem. Soc., Perkin Trans. 2*, 1979, 1115; A. J. Kirby, *Adv. Phys. Org. Chem.*, 1980, **17**, 183; L. Mandolini, *Adv. Phys. Org. Chem.*, 1986, **22**, 17.

2 I. B. Blagoeva, I. G. Pojarlieff and A. J. Kirby, *J. Chem. Soc., Perkin Trans. 2*, 1984, 745; J. R. Knowles, *Ann. Rev. Biochem.*, 1989, **58**, 195.

3 I. B. Blagoeva, D. T. Tashev and A. J. Kirby, *J. Chem. Soc., Perkin Trans. 1*, 1989, 1157.

4 I. B. Blagoeva, I. G. Pojarlieff and V. I. Rachina, *J. Chem. Soc., Chem. Commun.*, 1986, 946.

5 N. J. Leonard, *J. Am. Chem. Soc.*, 1949, **71**, 3094.

6 K. Maurer and E. H. Woltersdorf, *Z. Physiol. Chem.*, 1938, **254**, 23.

7 E. Gansser, *Z. Physiol. Chem.*, 1909 **61**, 32; *Chem. Abstr.*, 1910, **3**, 2705; *Chem. Zentralblatt*, 1909, **80**, 688.

8 V. Machácek, G. Svobodová and V. Šterba, *Collect. Czech. Chem. Commun.*, 1987, **52**, 140.

9 H. T. Huang, *J. Am. Chem. Soc.*, 1956, **78**, 2390.

10 J. Kaválek, V. Šterba and S. El Bahaie, *Collect. Czech. Chem. Commun.*, 1983, **48**, 1753.

11 (*a*) R. S. Brown, A. J. Bennet and H. Slebocka-Tilk, *Acc. Chem. Res.*, 1992, **25**, 481; H. Slebocka-Tilk, A. J. Bennet, J. W. Keillor, R. S. Brown, J. P. Guthrie and A. Jodhan, *J. Am. Chem. Soc.*, 1990, **112**, 8507; (*b*) A. J. Bennet, H. Slebocka-Tilk, R. S. Brown, J. P. Guthrie and A. Jodhan, *J. Am. Chem. Soc.*, 1990, **112**, 8497.

12 (*a*) A. C. Satterthwait and W. P. Jencks, *J. Am. Chem. Soc.*, 1974, **96**, 7018; (*b*) A. J. Kirby, T. G. Mujahid and P. Camilleri, *J. Chem. Soc., Perkin Trans. 2*, 1978, 1610; I. M. Kovach, M. Belz, M. Larsen, S. Rousy and R. L. Schowen, *J. Am. Chem. Soc.*, 1985, **107**, 7360; (*c*) C. C. Yang and W. P. Jencks, *J. Am. Chem. Soc.*, 1988, **110**, 2972.

13 S. Capasso, L. Mazzarella, F. Sica, A. Zagari and S. Salvadori, *J. Chem. Soc., Perkin Trans. 2*, 1993, 679.

14 M. N. Khan and J. E. Ohayagha, *J. Phys. Org. Chem.*, 1991, **4**, 547.

15 (*a*) G. L. Schmir, *J. Am. Chem. Soc.*, 1968, **90**, 3478; A. Cipiciani, P. Linda and G. Savelli, *J. Heterocycl. Chem.*, 1978, **15**, 1541; R. Pascal, D. Chauvey and R. Sola, *Tetrahedron Lett.*, 1994, **35**, 6291; ref. 12.

16 D. F. Detar, *J. Am. Chem. Soc.*, 1982, **104**, 7205.

17 In a different context see D. G. Oakenfull and W. P. Jencks, *J. Am. Chem. Soc.*, 1971, **93**, 178.

18 A. Williams, *Chem. Soc. Rev.*, 1994, 94.

19 E. Ware, *Chem. Rev.*, 1950, **46**, 403.

20 A. H. Koedjikov, I. B. Blagoeva, I. G. Pojarlieff and A. J. Kirby, unpublished results.

21 J. P. Fox and W. P. Jencks, *J. Am. Chem. Soc.*, 1974, **96**, 1436.

22 P. J. Taylor, *J. Chem. Soc., Perkin Trans. 2*, 1993, 1423.

23 O. S. Tee, M. Trani, R. A. McClelland and N. E. Seaman, *J. Am. Chem. Soc.*, 1982, **104**, 7219.

24 D. G. Oakenfull, K. Slavesen and W. P. Jencks, *J. Am. Chem. Soc.*, 1971, **93**, 188.

25 R. L. Schowen, *Prog. Phys. Org. Chem.*, 1972, **9**, 275.

26 K. B. J. Schowen in *Transition States of Biochemical Processes*, eds. R. D. Gandour and R. L. Schowen, Plenum Press, New York, 1978, p. 225.

27 M. Eigen, *Angew. Chem., Int. Ed. Engl.*, 1964, **3**, 1.

28 A. H. Koedjikov, I. B. Blagoeva, I. G. Pojarlieff and E. J. Stankevic, *J. Chem. Soc., Perkin Trans. 2*, 1984, 1077.

Paper 6/01831I
Received 15*th March* 1996
Accepted 30*th May* 1996